A reactive force-field (ReaxFF) Monte Carlo study of surface enrichment and step structure on yttria-stabilized zirconia

ARTICLE *in* SURFACE SCIENCE · AUGUST 2010

Impact Factor: 1.93 · DOI: 10.1016/j.susc.2010.05.006

4 AUTHORS, INCLUDING:

Matthias Batzill
University of South Florida
116 PUBLICATIONS **4,335** CITATIONS
SEE PROFILE

Adri C.T. van Duin
Pennsylvania State University
361 PUBLICATIONS **8,150** CITATIONS
SEE PROFILE

Surface Science 604 (2010) 1438–1444

Contents lists available at ScienceDirect

Surface Science

journal homepage: www.elsevier.com/ locate/susc

A reactive force-field (ReaxFF) Monte Carlo study of surface enrichment and step structure on yttria-stabilized zirconia

Adam D. Mayernick [a], Matthias Batzill [b], Adri C.T. van Duin [c,*], Michael J. Janik [a,*]

[a] Department of Chemical Engineering, Pennsylvania State University, University Park, PA 16802, United States
[b] Department of Physics, University of South Florida, Tampa, FL 33620, United States
[c] Department of Mechanical and Nuclear Engineering, Pennsylvania State University, University Park, PA 16802, United States

ARTICLE INFO

Article history:
Received 21 December 2009
Accepted 5 May 2010
Available online 19 May 2010

Keywords:
Yttria-stabilized zirconia
Reactive force-field
Monte Carlo
Surface enrichment
Simulated annealing
Density functional theory

ABSTRACT

To investigate surface segregation in yttria-stabilized zirconia (YSZ), DFT energies describing surface energy as a function of yttrium lattice position were used to parameterize a reactive-force field (ReaxFF). We used ReaxFF to perform Monte Carlo (MC) simulated annealing to sample structural configurations of flat YSZ (111) and vicinal YSZ (111) stepped surfaces. We evaluated yttrium surface segregation, oxygen vacancy position, and surface step composition for flat and stepped YSZ surfaces. It is thermodynamically favorable for yttrium atoms to segregate to the surface of YSZ, and specifically to step edge sites. Surface saturation of yttrium occurs at approximately 40% (40:60 Y:Zr ratio) while yttrium concentration at the step edge does not approach a saturation value, suggesting that steps on the YSZ surface are mainly yttria-terminated. We found that it is thermodynamically favorable for oxygen vacancies to occupy positions in the subsurface layer of YSZ, and a higher fraction of vacancies occupy positions NN to Y than NN to Zr. Yttrium segregation to step edges on the YSZ surface does not lower the surface formation energy of the stepped surface below that of the flat (111) termination, suggesting that the stability of YSZ surface steps observed experimentally is due to kinetic barriers for surface re-ordering.

1. Introduction

Yttria-stabilized zirconia (YSZ) is a mixed metal oxide which exhibits ionic conductivity at high temperatures, motivating the use of YSZ in oxygen sensors [1], supported catalysis [2,3], and as an electrolyte in solid-oxide fuel cells (SOFC) [4,5]. The addition of approximately 4–7 mol% yttria (Y_2O_3) to zirconia (ZrO_2) stabilizes the cubic phase of zirconia and results in the presence of oxygen vacancies [6]. These oxygen defects increase oxygen mobility with respect to ZrO_2, evidenced by the ionic conductivity of YSZ at high temperatures. The specific morphology and composition of the YSZ surface impacts functionality in each of the applications listed above. Characterization of YSZ surfaces by X-ray photoelectron spectroscopy (XPS) [7–9] and secondary ion mass spectrometry (SIMS) [10] methods indicates surface segregation of yttrium, suggesting that perturbations of the ZrO_2 surface structure may occur even at low bulk yttria content.

To investigate the surface behavior of YSZ-materials, we have to first consider the YSZ bulk structure. The cubic fluorite phase of pure zirconia is stable only at high temperatures (>2500 K) relative to monoclinic or tetragonal phases, however the addition of low valency dopants such as yttrium stabilizes the fluorite phase at temperatures as low as room temperature [8]. The addition of Y_2O_3 to ZrO_2 results in an oxygen-deficient cubic fluorite phase in which oxygen vacancies facilitate oxygen ion mobility sufficiently to provide ionic conductivity at high temperatures (>625 K) [11–13]. This oxygen deficient phase contains a distribution of yttrium, zirconium, and oxygen atoms for which the lowest energy configuration is difficult to characterize experimentally. The complex structure of this mixed metal oxide has resulted in conflicting data addressing the position of oxygen vacancies within the YSZ lattice. X-ray absorption studies of bulk YSZ have indicated that vacancies may be nearest neighbor (NN) to Zr^{4+} [14,15], while other such studies have indicated that vacancies may be nearest neighbor to Y^{3+} [16,17]. The configuration of yttrium, zirconium, oxygen atoms and oxygen defects is thus not conclusively characterized for bulk YSZ. The distribution of Y dopants and oxygen vacancies in bulk YSZ has previously been examined using reactive force field (ReaxFF) methods. This study showed that the oxygen coordination numbers (c.n.) of Zr and Y atoms in bulk YSZ-14 (1:3 Y:Zr ratio) are 6.9 and 7.9, respectively, implying that oxygen vacancies in bulk YSZ are NN to Zr^{4+} [18].

The structural details of YSZ surfaces are also difficult to elucidate experimentally, where the composition may differ significantly from the bulk. Characterization of YSZ surfaces has indicated that the yttrium composition is increased with respect to bulk concentration [7,8,10], and that corrugated surfaces containing a high density of steps may be stable relative to flat YSZ surfaces or kinetically inhibited

* Corresponding authors. Janik, is to be contacted at 104 Fenske Laboratory, University Park, PA 16802, United States. Tel.: +1 814 863 9366; fax: 1 814 865 7846. Duin, 136 Research Building East, University Park, PA 16802, United States. Tel.: +1 814 863 6277; fax: +1 814 865 3389.
E-mail addresses: acv13@psu.edu (A.C.T. van Duin), mjanik@psu.edu (M.J. Janik).

0039-6028/$ – see front matter © 2010 Elsevier B.V. All rights reserved.
doi:10.1016/j.susc.2010.05.006

from annealing [9,19,20]. X-ray photoelectron spectroscopy (XPS) studies on YSZ surfaces have indicated that yttrium segregates to the YSZ surface and that the surface Y content may be increased more than two-fold with respect to the bulk Y concentration [7–9]. Lahiri et al. used angle-dependent XPS analysis to conclude that the YSZ (111) surface of 10% Y bulk YSZ (Y:Zr = 10:90) is comprised of either a yttrium-enriched top layer at 45% yttrium (Y:Zr = 45:55) or an enriched top two layers at 30% yttrium (Y:Zr = 30:70) [9]. Auger electron spectroscopy, low-energy electron diffraction (LEED), and SIMS experiments have also indicated yttrium enrichment of the YSZ (100) and (110) terminations [10]. Despite numerous methods for characterizing the composition of YSZ surfaces, direct imaging with electron microscopy techniques is challenged by the electron insulating properties of YSZ. Atomic force microscopy (AFM) studies have indicated that the stable morphology of the YSZ (100) termination is composed of a series of parallel steps [19], however AFM images cannot achieve atomic level resolution. The first scanning tunneling microscopy (STM) images of the YSZ (111) surface indicate the presence of monatomic steps before and after annealing at 1000 K and ion sputtering [9,20]. These results suggest that a highly stepped YSZ termination may be stable relative to a flat surface, however step composition and the surface thermodynamics of step formation are poorly understood.

Computational chemistry approaches to modeling oxide surfaces can investigate structural details which can be difficult to characterize experimentally, and provide insight into the electronic structure at the surface. Density functional theory (DFT) methods provide the means to directly calculate surface formation energies and evaluate the thermodynamic stability of surfaces with different geometry and composition. Previous DFT studies of the surfaces of YSZ have focused on evaluating the thermodynamic stability [21,22] and catalytic activity [3] of YSZ surfaces. Wang et al. [22] used DFT methods to show that it is thermodynamically favorable for yttrium atoms to segregate to the subsurface layer of YSZ (111). The computational intensity of DFT calculations challenges the evaluation of the multitude of configurations of yttrium atoms and oxygen vacancies possible on a YSZ surface. Catlow et al. [23] used interatomic potential-based methods to calculate segregation energies of yttrium for flat YSZ surfaces and showed that yttrium segregation to the YSZ (111) surface is exothermic. No previous computational study has addressed corrugated YSZ surfaces and evaluated the thermodynamic stability or composition of stepped surface morphologies. To evaluate the structure and composition of vicinal YSZ (111) surfaces with monatomic steps, it is necessary to implement a computational methodology which samples surface configurations of oxygen, metal atoms, and defects within an energy minimization scheme. This methodology must also permit the use of large surface models (>1000 atoms) relative to DFT calculations (~100–200 atoms) to accurately represent the heterogeneity of stepped surface structures.

Herein, we describe the results of a combined DFT and reactive force field (ReaxFF) based Monte Carlo study, aiming to calculate the surface formation energy of flat and stepped ZrO_2 and YSZ (111) surfaces. We use DFT energies to extend an existing YSZ-ReaxFF reactive force field [18] and perform Monte Carlo (MC) simulated annealing to sample structural configurations of flat YSZ (111) and vicinal YSZ (111) stepped surfaces. The use of ReaxFF allows for the consideration of larger stepped surface models, and the MC simulations we report facilitate greater sampling of possible surface configurations and compositions than is computationally tractable with DFT methods. Our ReaxFF-MC approach allows yttrium and zirconium atoms as well as oxygen atoms and oxygen vacancies to swap lattice positions while continuously performing local structure energy minimization. Using this methodology we lower the temperature until we have reached a minimum energy configuration for each surface model, and determine the optimum surface composition. We evaluate yttrium surface segregation, oxygen vacancy position, and surface step composition for flat and stepped YSZ surfaces. We show that it is thermodynamically favorable for yttrium atoms to segregate to the surface of YSZ, and specifically to step edge sites. It is thermodynamically favorable for oxygen vacancies to occupy positions in the subsurface layer of YSZ, and a higher fraction of vacancies occupy positions NN to Y than NN to Zr.

2. Methods

2.1. Electronic structure method

Quantum-chemical calculations were carried out using the Vienna Ab-initio Simulation Program (VASP), an ab-initio total-energy and molecular dynamics program developed at the Institute for Material Physics at the University of Vienna [24–26]. The projector augmented wave (PAW) method [27] was used to represent the core region, with valence electron wavefunctions expanded in a tractable plane wave basis set (with an energy cutoff of 450 eV, all calculations spin-polarized). Valence configurations were $4s^2 4p^6 4d^2 5s^2$ for zirconia, for oxygen $2s^2 2p^4$, and for Y $4s^2 4p^6 4d^2 5s^1$. The Brillouin zone was sampled using a $(2\times2\times2)$ Monkhorst Pack (MP) grid [28] for bulk zirconia, and a $(2\times2\times1)$ MP grid for surfaces, with the third vector perpendicular to the surface. Structural optimizations were performed by minimizing the forces on all atoms to below 0.05 eV $Å^{-1}$. The Perdew–Wang (PW91) version of the generalized gradient approximation (GGA) is used to incorporate exchange and correlation energies [29].

2.2. Model construction

Fig. 1 displays the top (a) and side (b) views of the flat ZrO_2 surface cell, with the cell length and cell width defined. The optimized equilibrium lattice parameter of cubic zirconia is 5.127 Å, which is within 1% of the reported experimental value of 5.090 Å [30]. The ZrO_2/YSZ (111) surface is modeled as a slab of cubic fluorite ZrO_2 separated by 15 Å of vacuum in the direction perpendicular to the surface. Fig. 1 displays the slabs used to model the flat and stepped ZrO_2 surfaces, for each expansion of the surface unit cell. Slabs of different cell width and length are used to model the ZrO_2 flat and stepped surfaces to consider different surface yttrium and oxygen vacancy concentrations, as well as different concentrations of step edges. For each stepped surface slab, the step is constructed from the flat surface by removing ZrO_2 surface rows to form a single ZrO_2 unit plateau on the (111) surface. Similar models of (111) plateaus were used in DFT models to represent steps on cubic fluorite CaF_2 [31]. The step width for each stepped surface slab is set at 3 ZrO_2 units to allow yttrium placement at either side or in the middle of the non-symmetric plateau. Structural optimizations were performed allowing the top ZrO_2 layer (which includes only atoms in the plateau for stepped surfaces) to relax, and also allowing the top two layers to relax (which includes both atoms in the plateau and the ZrO_2 layer beneath the plateau for stepped surfaces). Structural optimizations were performed with yttrium atoms substituted into the surface layer as well as subsurface layer of ZrO_2, and oxygen vacancies in varying lattice positions with respect to the surface and with respect to yttrium atoms. For each DFT calculation, yttrium atoms were substituted for Zr atoms as pairs with one oxygen vacancy per Y_2 pair to obtain the stoichiometry of ZrO_2/Y_2O_3. Yttrium atoms were substituted into and oxygen atoms were removed from the zirconia lattice at the surface sites detailed in Fig. 1(d) for each stepped surface model. Each slab model was mirrored to avoid spurious dipole interactions between slabs that may occur for slabs containing oxygen vacancies within the periodic model. The largest DFT unit cell considered in this study included 144 atoms, and required 102 h of run time on 16 3.0 GHz Intel Xeon E5472 (Woodcrest) Quad-Core Processors to perform structural optimization.

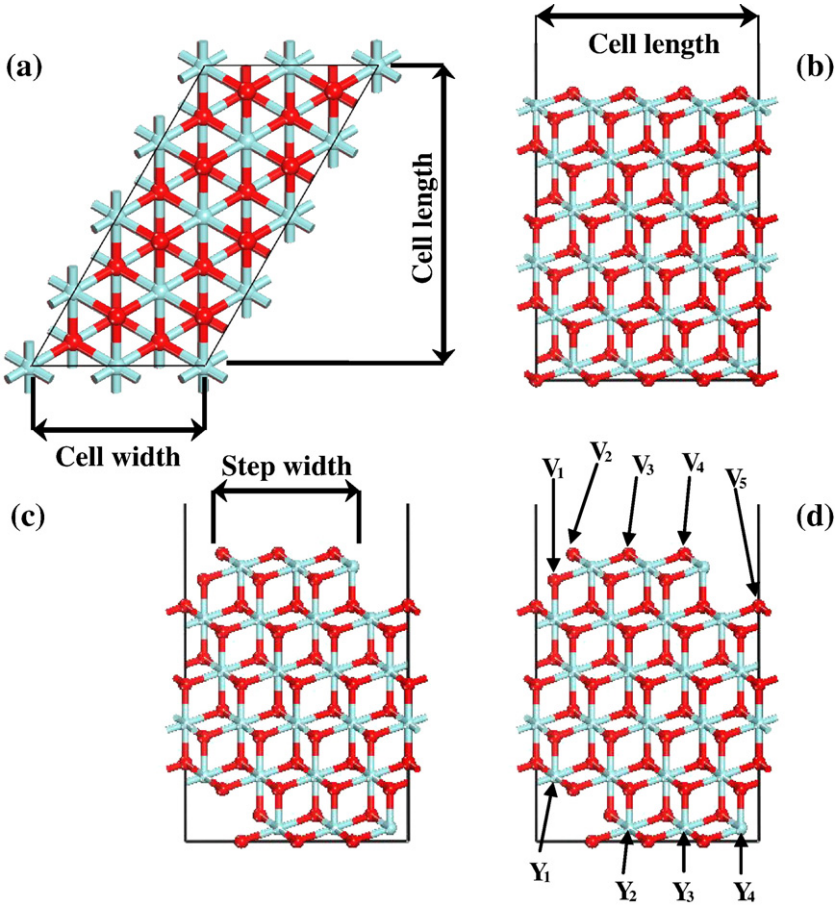

Fig. 1. DFT slab models of (a) ZrO_2 (111) surface (top view), (b) ZrO_2 (111) surface (side view), and (c), (d) stepped ZrO_2 (111) surface. Cell length and cell width are defined in (a) and (b), step width in (c), and oxygen vacancy sites (V_x) and yttrium doping sites (Y_x) in (d).

2.3. Calculation of surface formation free energies

To compare relative energies between flat and stepped surfaces of different sizes and configuration, we calculate the surface formation energy:

$$\Delta G_{surf} = \frac{E_x - \left(n_{ZrO_2} \cdot \mu_{ZrO_2} + n_{Y_2O_3} \cdot \mu_{Y_2O_3}\right)}{2 \cdot A_{slab}} \quad (1)$$

where A_{slab} is the surface area of the mirrored surface slab, $\mu_{ZrO_2}$and $\mu_{Y_2}O_3$ are the bulk chemical potentials of zirconia and yttria, respectively, E_x is the DFT energy of the surface slab, and n_{ZrO_2} and $n_{Y_2}O_3$ are the number of formula units of zirconia and yttria in the slab, respectively. Bulk solid chemical potentials are taken from optimized DFT structures, and therefore neglect entropic and enthalpic (T) corrections, consistent with the treatment of surface structures [32,33]. To validate that yttrium and oxygen vacancy distributions will be dominated by potential energy differences, vibrational frequencies associated with an O atom in the bulk and at the step of ZrO_2 were approximated through construction of a constrained Hessian. The vibrational entropy difference is 9×10^5 eV $Å^{-1}$, for a TS difference of 0.15 eV at 1750 K. This value is small compared to the DFT 1.31–2.54 eV difference calculated for various oxygen vacancy positions.

2.4. ReaxFF methodology

2.4.1. ReaxFF force field development

ReaxFF is a bond-order based force field, allowing for the formation and dissociation of chemical bonds during a simulation [34]. ReaxFF combines a continuous bond order with a polarizable charge calculation, which enables application of ReaxFF to covalent, metallic and ionic materials. The ReaxFF force field was earlier parameterized to describe the structure and interactions in bulk YSZ-materials [18]. This earlier YSZ-ReaxFF description matched the equation of state for bulk YSZ as well as for metallic Y and Zr phases, monoclinic, tetragonal, and cubic ZrO_2 and cubic Y_2O_3 [18]. The DFT optimizations described in the previous section were used to re-parameterize this force field to accurately model the YSZ (111) surface. The force field was parameterized to specifically match the DFT calculated energy differences for yttrium surface segregation and oxygen vacancy position. Table 1 displays the energy differences which were most highly weighted in the parameterization of the ReaxFF force field. The full training set of DFT values which were used to parameterize the ReaxFF force field for accurate description of YSZ surfaces can be found in the supplementary information. The ReaxFF force field file used herein is included in the Supplementary information, and is compatible with the open-source LAMMPS code as well as the stand-alone ReaxFF code (available upon request from corresponding author van Duin). The values displayed in

Table 1
Energy differences for yttrium and oxygen vacancy location at the YSZ (111) surface calculated by ReaxFF and DFT.

YSZ (111)	(eV)		
Energy difference	Ffield *E*	DFT *E*	*E* difference
$(Y_{surf}) - (Y_{subsurf})$	−1.31	−1.27	+0.04
(Vac NN to Zr_{surf}) − (Vac NN to Y_{surf})	−1.95	−2.11	−0.16
(Vac NN to Zr_{surf}) − (Vac NN to $Zr_{subsurf}$)	−1.50	−1.00	+0.51
(Vac NN to Zr_{surf}) − (Vac NN to $Y_{subsurf}$)	−2.54	−2.57	−0.03

Table 1 are for the flat YSZ (111) surface, and confirm the preference for yttrium to occupy surface sites and oxygen vacancies to prefer surface sites nearest neighbor (NN) to Zr atoms.

2.4.2. Monte Carlo simulated annealing with ReaxFF

The ReaxFF Monte Carlo Reactive Dynamics Method was developed to resolve partial or mixed occupation of crystallographic sites of mixed metal oxides and previously applied to the system of MO_3VO_x [35]. Monte Carlo (MC) simulations were performed to sample possible surface configurations for yttrium and oxygen vacancy concentration and locate minimum energy geometries. Interchange of the lattice positions of Y and Zr atoms or oxygen atoms and oxygen vacancies was performed, followed by re-optimization of the system energy. A Metropolis criteria was used to determine whether the interchange (and thus the new structure) was allowed. Oxygen vacancies were represented as weakly interacting atoms which were allowed to occupy oxygen lattice positions, for which our method includes a weak Van der Waals (VDW) interaction with the surrounding lattice and weak repulsion between vacancies. This method of describing oxygen vacancies permits swapping of oxygen and oxygen vacancies to determine optimum vacancy position while the weak VDW interaction between vacancies and other atoms prevents dissociation of vacancies from the YSZ surface.

Mirrored slabs of pure and Y-doped ZrO_2 were constructed to model the vicinal YSZ (111) surface, separated by 15 Å in the *z*-direction. Fig. 2 displays a stepped slab model used in our ReaxFF Monte Carlo simulations. The stepped YSZ (111) surface was modeled by vicinal surface slabs of termination (10 10 8), with one step on each side of the slab. The (10 10 12) termination was also considered, however its surface formation energy is greater than that of (10 10 8) due to lower coordination numbers for edge atoms at the step edge. Surface and step edge sites are labeled in Fig. 2 as they are referred to in this study. The total yttrium concentration in our slab model was varied to evaluate the trend in surface and step composition with respect to bulk yttrium content. To investigate the dependence of yttrium surface segregation on the YSZ bulk:surface ratio (which represents the relative size of the bulk "yttrium reservoir"), simulations were performed using different slab thicknesses.

Simulated annealing Monte Carlo simulations were performed by cooling from 1750 K to 250 K in 250 K intervals with 10,000 MC steps at each temperature to ensure convergence with respect to total system energy. This simulated annealing cycle was performed *n* times for each initial composition studied herein, each time beginning with the same initial structure. The values reported for surface site composition in Section 3.2 are the mean values over all *n* repetitions for each model. Error for each surface site composition is estimated by the 95% confidence interval of the mean:

$$95\%C.I. = 1.96 \cdot \frac{\sigma}{\sqrt{n}} \tag{2}$$

where σ is the standard deviation of the compositions calculated for all repetitions, and *n* is the number of MC repetitions. The number of MC repetitions $n = 49$ for our thinnest slab as shown in Fig. 2, and $n = 25$ for all other slab thicknesses considered. The number of MC repetitions *n* used for each model was chosen to ensure convergence of the mean and standard deviation of the mean of each surface site composition with respect to *n*, and to achieve error bars small enough to make qualitative comparisons between data sets. The largest ReaxFF unit cell considered in this study included approximately 2200 atoms, and required 62 h of run time on one 3.0 GHz Intel Xeon E5472 (Woodcrest) Quad-Core Processor to complete one MC annealing cycle.

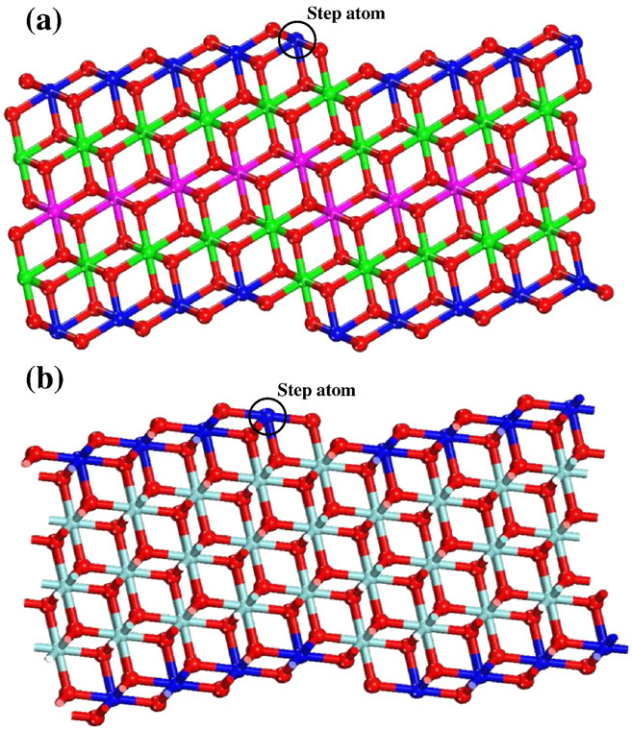

Fig. 2. (a) Thinnest ReaxFF slab model of the (10 10 8) YSZ surface with blue atoms corresponding to surface metal atoms, green atoms as 2nd layer metal atoms, purple atoms as third layer metal atoms and red atoms as oxygen. (b) ReaxFF slab model of the (10 10 12) YSZ surface with blue atoms corresponding to surface metal atoms.

3. Results and discussion

3.1. DFT surface energies of YSZ (111)

Surface formation energies indicate that the stepped YSZ (111) surface has a higher surface energy than the flat (111) surface. Table 2 displays the DFT surface formation energies for the largest DFT models considered of flat and stepped ZrO_2 and YSZ (111) surfaces. The complete set of DFT structures and their surface formation energies are available as supplementary information. The surface energy for the flat YSZ surface listed in Table 2 is that of the lowest energy surface configuration, for which the one oxygen vacancy included in the unit cell is located nearest neighbor (NN) to surface zirconium atoms. This data shows that the formation energy of the flat YSZ (111) surface is less than that of the pure zirconia (111) surface. The surface formation energy of the stepped YSZ (111) surface is larger than that of pure zirconia, and is dependent on the relative positions of yttrium and oxygen vacancies. The size limitations required for a tractable DFT calculation necessitate the use of an asymmetric slab model, and the stability of the two different step configurations cannot be independently evaluated. Furthermore, the small 3 MO_2 unit width of the step allows for minimal sampling of possible yttrium and oxygen vacancy configurations and limits the conclusiveness of the DFT results.

Table 2
Surface formation energies for the cubic fluorite ZrO_2 and YSZ (111) surfaces calculated by DFT. Yttrium and oxygen vacancy positions within the step model are noted as labeled in Fig. 1(d).

System	Surface energy (eV/Å^2)
ZrO_2_flat	0.05
YSZ_flat	0.04
ZrO_2	0.08
YSZ_Y_1_V_5	0.10
YSZ_Y_2_V_2	0.09
YSZ_Y_3_V_3	0.08
YSZ_Y_4_V_4	0.09

3.2. ReaxFF Monte Carlo simulated annealing

3.2.1. Step edge and surface composition as a function of bulk yttrium concentration

The surface and step edge yttrium content was evaluated by calculating the percentage of surface and step edge metal sites occupied by yttrium atoms,

$$site\ Y\% = \left(\frac{\#\ of\ "x"\ sites\ occupied\ by\ Yttrium}{total\ \#\ of\ "x"\ sites}\right) \cdot 100 \quad (3)$$

where x refers to either "step edge," "surface," "2nd layer" (1st subsurface layer), or "3rd layer" (2nd subsurface layer) sites. The bulk yttrium content (bulk Y%) in our models is similarly defined as the ratio of yttrium atoms to total metal atoms. Fig. 3 displays the site Y% for the vicinal (10 10 8) YSZ surface calculated from our MC simulations for our thinnest slab model (Fig. 2(a)), for 8, 10, and 12% bulk Y%. The larger error bars for the step Y% reflect the lesser number of step sites in the slab model as compared to the number of surface sites (1:9 step:surface site ratio).

It is thermodynamically favorable for yttrium atoms to segregate to the surface of YSZ, and specifically to step edge sites. Yttrium surface content increases as bulk content increases, and in all compositions from 8% bulk Y% to 12% bulk Y% the surface content exceeds that of the bulk. The step edge site%Y exceeds both the bulk%Y as well as the surface site Y%. This data shows that yttrium atoms specifically segregate to step edge sites on the YSZ surface, and that the concentration of yttrium at step edge and surface sites increases as bulk yttrium concentration increases.

3.2.2. Yttrium step edge and surface saturation

To evaluate the dependence of yttrium segregation on the size of the bulk "yttrium reservoir," we performed MC annealing runs on thicker (10 10 8) slabs with 10% bulk Y%. Fig. 4 displays the percentage of metal sites occupied by yttrium at the step edge, surface, and subsurface layers of YSZ versus slab thickness. The slab thickness is normalized to the thinnest slab considered (Fig. 2(a)). In most experimental systems, the macroscopic depth of YSZ provides for a substantial reservoir of bulk yttria that may segregate to the surface. Therefore, the computational results should be extrapolated to infinite thickness for comparison with the experimental system. The concentration of yttrium at the step edge exceeds that of the bulk as

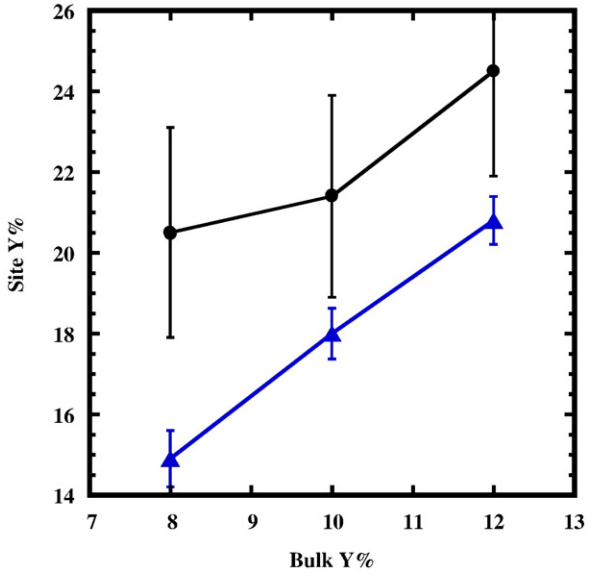

Fig. 3. Y% at the step edge (●) and surface (▲) on the YSZ surface as a function of bulk yttrium concentration.

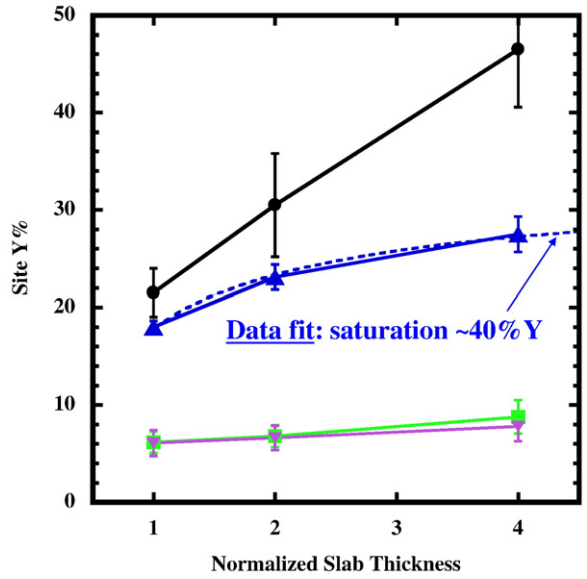

Fig. 4. Y% at the step edge (●), surface (▲), 2nd surface layer (■), and 3rd surface layer (▼) on the YSZ surface as a function of slab thickness.

well as the surface for each slab thickness considered. The concentration of yttrium at the surface also exceeds that of the bulk as well as the second and third subsurface layers. Yttrium enrichment of the surface begins to approach a saturation point at which the change in surface Y% with respect to slab thickness reaches zero. This result shows that if the bulk:surface ratio of YSZ is large enough, yttrium enrichment of the surface will saturate at a concentration less than that at the step edge. Lahiri et al. report angle-dependent XPS results which suggest that the surface saturation point occurs at 45% yttrium if only the surface layer is yttrium enriched [9]. Our simulations show that yttrium enrichment only occurs in the surface layer of YSZ and we estimate this saturation point at ~40% yttrium (using a $A-\frac{B}{\sqrt{\tau}}$ data fit for the surface Y%, where τ is the normalized slab thickness). The concentration of yttrium at the step edge does not approach a saturation level, however, suggesting that steps on the YSZ surface are mainly yttria-terminated. The result that YSZ step edges are mainly yttria-terminated is in agreement with the fact that the selectivity for formic acid decomposition of the YSZ surface is similar to that of pure Y_2O_3 [9].

We also calculate surface and step Y% for the (10 10 12) YSZ termination (shown in Fig. 2(b)) to evaluate the dependence of yttrium segregation on step structure. We calculate the step Y% and surface Y% as 10.9% ± 5.04 and 17.6% ± 1.54, respectively for the (10 10 12) YSZ termination for a slab of the thickness displayed in Fig. 2(b) (the same thickness as the thinnest slab considered for the (10 10 8) termination). These values for step and surface Y% on the (10 10 12) termination indicate the opposite trend in yttrium segregation to step and surface sites as compared to the (10 10 8) termination. This result illustrates that yttrium segregation to the step edge is dependent on the structure and coordination environment of the step edge sites. The majority of our calculations have utilized the (10 10 8) termination as this surface has a lower surface formation energy than the (10 10 12) termination, and thus YSZ step edges are more likely to be terminated as shown in our (10 10 8) slab model.

3.2.3. Distribution of yttrium, zirconium, oxygen and oxygen vacancies

To evaluate the distribution of yttrium, zirconium, oxygen and oxygen vacancies, we calculate the atomic radial pair distribution function $g(r)$:

$$g(r) = \frac{n(r)}{\rho \cdot 4\pi r^2 \cdot \Delta r} \quad (4)$$

Table 3
Coordination numbers of oxygen and oxygen vacancies ($V_O^{\bullet\bullet}$) for Zr and Y atoms in the overall YSZ slab and for Zr and Y atoms in the surface layer.

Pair	Overall (*c.n.*)	Surface (*c.n.*)
Zr–O	6.99	5.92
Zr–$V_O^{\bullet\bullet}$	0.15	0.21
Y–O	6.38	5.74
Y–$V_O^{\bullet\bullet}$	0.39	0.32

Table 4
Oxygen vacancy concentration in different regions of the YSZ surface slab.

Region	Vacancy concentration
Step edge	2.85% ± 1.61
Surface layer	2.64% ± 0.68
Subsurface layer	7.27% ± 1.35
Entire slab	2.50% ± 0.00

where $n(r)$ is the number of atoms within Δr at distance r with respect to a central atom, and ρ is the bulk density. The values of $g(r)$ that we calculate are the averages for the x output structures of MC simulated annealing for each surface model. We use $g(r)$ to calculate the coordination number (*c.n.*):

$$(c.n.) = \int_0^{r_1} \left[\rho \cdot 4\pi r^2 \cdot g(r)\right] dr \tag{5}$$

where r_1 is the radial distance from each atom at the first minimum of $g(r)$, and (*c.n.*) represents the number of atoms in the first coordination shell of the central atom. Both $g(r)$ and (*c.n.*) are calculated for the atom pairs of Zr–O, Y–O, Zr–$V_O^{\bullet\bullet}$, and Y–$V_O^{\bullet\bullet}$ for each surface model. The $g(r)$ plots are included as supplementary information, and the coordination numbers calculated from these are given in Table 3.

Table 3 displays the overall (*c.n.*) calculated for each pair for the thickest slab model with 10% yttrium, as well as the (*c.n.*) for Y and Zr atoms in the surface layer only. Zirconium atoms in bulk cubic fluorite ZrO_2 are eight-fold oxygen coordinate, whereas we calculated an average oxygen (*c.n.*) of 6.99 because our model includes zirconium atoms at under-coordinated surface sites as well as oxygen vacancies. The average coordination number for Y atoms is 6.38, less than that of Zr atoms. The lower coordination of yttrium relative to zirconium is due to two factors: (1) a higher percentage of the yttrium atoms relative to zirconium atoms in each unit cell occupy surface sites versus bulk lattice positions and (2) the $V_O^{\bullet\bullet}$ (*c.n.*) for Y is greater than the $V_O^{\bullet\bullet}$ (*c.n.*) for Zr over the entire slab as well as in the surface layer. The overall $V_O^{\bullet\bullet}$ (*c.n.*) for Zr and Y are 0.15 and 0.39, respectively, showing that a higher percentage of oxygen vacancies are located NN to Y than Zr. This distribution of oxygen vacancies differs from the previous ReaxFF study of bulk YSZ [18], indicating a difference in vacancy position in layers near the YSZ surface versus the bulk. The $V_O^{\bullet\bullet}$ (*c.n.*) for Zr and Y in the surface layer are 0.21 and 0.32, respectively, indicating that there is shift in the distribution of oxygen vacancies at the YSZ surface towards a higher fraction of vacancies occupying sites NN to Zr.

To differentiate between oxygen vacancies at the YSZ surface, in the subsurface layer (both of which contribute to the (*c.n.*) for Y and Zr atoms in the surface metal layer), and coordinated to step edge atoms, we calculate the oxygen vacancy concentration at topmost (surface), the 2nd (subsurface) oxygen layers, and in the first coordination shell of step edge atoms. Table 4 displays the concentration of oxygen vacancies in the surface and subsurface layers and at the step edge. The concentration of oxygen vacancies at the YSZ surface and step edge is similar to that of the entire slab, however the concentration of oxygen vacancies in the subsurface layer is nearly three times greater than the overall composition. This result shows that it is thermodynamically favorable for oxygen vacancies to segregate to the subsurface layer in YSZ. The high concentration of subsurface oxygen vacancies also illustrates that the trends we observe in $V_O^{\bullet\bullet}$ (*c.n.*) for Y and Zr in the surface layer are dominated by subsurface oxygen vacancies.

3.2.4. Relative energy of flat and stepped YSZ surfaces

To evaluate the relative stability of steps on YSZ surfaces, we calculate the energy difference between the flat (111) surface and our vicinal stepped surface model for ZrO_2 and 10% bulk Y%. Fig. 5 displays the relative surface formation energies for flat and stepped pure zirconia and YSZ. The surface energy difference in Fig. 5 for ZrO_2 is calculated from the energies of flat and stepped zirconia surface models which have been structurally optimized using the conjugate-gradient method. The surface energy difference in Fig. 5 for YSZ is calculated as the average of energies of flat and stepped YSZ output structures from MC annealing

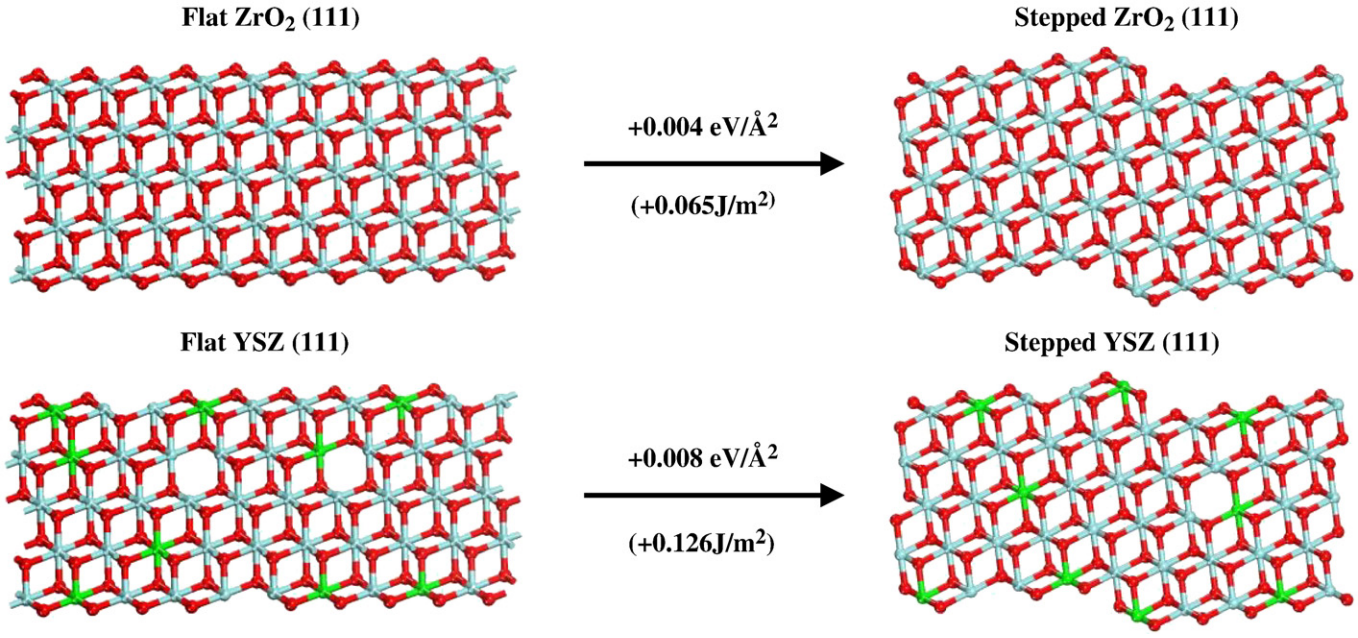

Fig. 5. Relative surface formation energies for flat and stepped pure zirconia (ZrO_2) and YSZ surfaces.

cycles, which have also been structurally optimized using the conjugate-gradient method. The energy differences between the ReaxFF flat surface and stepped surface models for both ZrO_2 and YSZ are much lower than the energy differences calculated in our DFT models, due to much lower step density in our ReaxFF models. The energies in Fig. 5 show that the vicinal stepped ZrO_2 surface has a higher surface formation energy than the flat ZrO_2 (111) surface, and that the energy difference between flat and stepped is less than that for YSZ. This result suggests that yttrium doping of zirconia does not stabilize step formation on the cubic zirconia surface and that the formation of surface steps is not thermodynamically favorable on pure zirconia or YSZ. The relative energy difference between a flat and stepped termination is low for both pure zirconia and YSZ, however, suggesting that in an experimental system steps may be present in varying concentration depending on sample preparation method.

4. Conclusions

We performed Monte Carlo (MC) simulated annealing, using a ReaxFF reactive force field based on DFT data describing YSZ surface energies, to sample structural configurations of flat YSZ (111) and vicinal YSZ (111) stepped surfaces. Yttrium surface segregation, oxygen vacancy position, and surface step composition for flat and stepped YSZ surfaces was evaluated. We observed that the specific termination of step edges influences yttrium segregation behavior, however yttrium atoms segregate to the surface and specifically to step edge sites for the low energy YSZ (111) vicinal stepped (10 10 8) surface. We found that surface saturation of yttrium occurs at approximately 40% (40:60 Y:Zr ratio), which is in agreement with XPS results which suggest that this saturation point occurs at 45% yttrium [9]. Our radial distribution function analysis indicates that it is thermodynamically favorable for oxygen vacancies to occupy positions in the subsurface layer of YSZ, and a higher fraction of vacancies occupy positions NN to Y than NN to Zr. Yttrium segregation to step edges on the YSZ surface does not lower the surface formation energy of the stepped surface below that of the flat (111) termination, and the formation of surface steps of the specific geometry considered herein is not thermodynamically favorable on pure zirconia or YSZ.

This study shows that the specific structure and morphology of the YSZ surface influences the surface segregation of yttrium. Stepped YSZ surfaces afford altered chemical functionality with respect to flat surfaces, as active step edge sites are mainly occupied by yttrium atoms. We demonstrate that our ReaxFF-MC methodology is a useful computational tool for evaluating the structure and composition of complex mixed metal oxide surfaces, for which direct consideration of lattice defects is necessary.

Acknowledgements

Acknowledgement is made to the Donors of the American Chemical Society Petroleum Research Fund #46724-G5 for support of this research.

Appendix A. Supplementary data

Supplementary data associated with this article can be found, in the online version, at doi:10.1016/j.susc.2010.05.006.

References

[1] J.S. Park, C.O. Park, H.J. Kim, N. Miura, Solid State Ionics 176 (2005) 1371.
[2] M. Itome, A.E. Nelson, Catal. Lett. 106 (2006) 21.
[3] M. Shishkin, T. Ziegler, J. Phys. Chem. C 112 (2008) 19662.
[4] M. Vogler, A. Bierberle-Hutter, L. Gauckler, J. Warnatz, W. Bessler, J. Electrochem. Soc. 156 (2009) B663.
[5] A. Martinez-Amesti, A. Larranaga, L.M. Rodriguez-Martinez, M.L. No, J.L. Pizarro, A. Laresgoiti, M.I. Arriortua, J. Electrochem. Soc. 156 (2009) B856.
[6] T.H. Etsell, S.N. Flengas, Chem. Rev. 70 (1970) 339.
[7] D. Majumdar, D. Chatterjee, Thin Solid Films (1991) 349.
[8] D. Majumdar, D. Chatterjee, J. App. Phys. 70 (1991) 988.
[9] J. Lahiri, A.D. Mayernick, S.L. Morrow, B.E. Koel, A.C.T. van Duin, M.J. Janik, M. Batzill, J. Phys. Chem. C (2009).
[10] G.S. Herman, M.A. Henderson, K.A. Starkweather, E.P. McDaniel, J. Vac. Sci. A. 17 (1999) 939.
[11] J. Nowotny, Solid State Ionics 49 (1991) 119.
[12] B.C.H. Steele, J. Power, Sources 49 (1994) 1.
[13] B.C.H. Steele, R.M. Dell, Philos. Trans.: Math., Phys., Eng. Sci. 354 (1996) 1695.
[14] C.R.A. Catlow, A.V. Chadwick, G.N. Greaves, L.M. Moroney, J. Am. Ceram. Soc. 69 (1986) 272.
[15] P. Li, I.-W. Chen, J. Penner-Hahn, J. Am. Ceram. Soc. 77 (1994) 118.
[16] M.H. Tuilier, J. Dexpert-Ghys, H. Dexpert, P. Lagarde, J. Solid State Chem. 69 (1987) 153.
[17] W.L. Roth, R. Wong, A.I. Goldman, E. Canova, Y.H. Kao, B. Dunn, Solid State Ionics 18 (1986) 1115.
[18] A.C.T. v. Duin, B.V. Merinov, S.S. Jang, W.A.G. III, J. Phys. Chem. A 112 (2008) 3133.
[19] T. Thome, L.P. Van, J. Cousty, J. Euro. Ceram. Soc. 24 (2004) 841.
[20] S.L. Morrow, T. Luttrell, A. Carter, M. Batzill, Surf. Sci. 603 (2009) L78.
[21] G. Ballabio, M. Bernasconi, F. Pietrucci, S. Serra, Phys. Rev. B 70 (2004) 075417.
[22] X.-G. Wang, Surf. Sci. Lett. 602 (2008) L5.
[23] X. Xia, R. Oldman, C.R.A. Catlow, Chem. Mater. 21 (2009) 3576.
[24] G. Kresse, J. Furthmuller, Comput. Mater. Sci. 6 (1996) 15.
[25] G. Kresse, J. Furthmuller, Phys. Rev. B 54 (1996) 11169.
[26] G. Kresse, J. Hafner, Phys. Rev. B 47 (1993) 558.
[27] G. Kresse, D. Joubert, Phys. Rev. B 59 (1999) 1758.
[28] H.J. Monkhorst, J.D. Pack, Phys. Rev. B 13 (1976) 5188.
[29] J.P. Perdew, J.A. Chevary, S.H. Vosko, K.A. Jackson, M.R. Pederson, D.J. Singh, C. Fiolhais, Phys. Rev. B 46 (1992) 6671.
[30] O. Ruff, F. Ebert, J. Inorganic and General Chem. 180 (1929) 252.
[31] T.G. Cooper, N.H.d. Leeuw, J. Mater. Chem. 13 (2002) 93.
[32] K. Reuter, M. Scheffler, Phys. Rev. B 65 (2001) 035406.
[33] A.D. Mayernick, M.J. Janik, J. Chem. Phys. 131 (2009).
[34] A.C.T. van Duin, S. Dasgupta, F. Lorant, W.A. Goddard III, J. Phys, Chem. A 105 (2001) 9396.
[35] K. Chenoweth, A.C.T. van Duin, W.A. Goddard III, Angew. Chem. Int. 48 (2009) 7630.